AD-A216 609

DTIC FILE COPY

1

REPORT DOCUMENTATION PAGE

Form Approved
OMB No. 0704-0188

1. AGENCY USE ONLY (Leave blank)	2. REPORT DATE	3. REPORT TYPE AND DATES COVERED
	September 1989	professional paper

4. TITLE AND SUBTITLE
DETECTION OF COVERT MESSAGE TRANSMISSIONS

5. FUNDING NUMBERS
In-house funding

6. AUTHOR(S)
R. A. Dillard and G. M. Dillard

7. PERFORMING ORGANIZATION NAME(S) AND ADDRESS(ES)
Naval Ocean Systems Center
San Diego, CA 92152-5000

8. PERFORMING ORGANIZATION REPORT NUMBER

9. SPONSORING/MONITORING AGENCY NAME(S) AND ADDRESS(ES)
Naval Ocean Systems Center
San Diego, CA 92152-5000

10. SPONSORING/MONITORING AGENCY REPORT NUMBER

11. SUPPLEMENTARY NOTES

12a. DISTRIBUTION/AVAILABILITY STATEMENT
Approved for public release; distribution is unlimited.

12b. DISTRIBUTION CODE

13. ABSTRACT (Maximum 200 words)

In this paper we describe and compare methods of detecting short, randomly occurring messages. The emphasis is on spread-spectrum transmissions, but the energy detection results also apply to simple burst communications, such as those used for interrogation or identification among network elements.

Accesion For	
NTIS CRA&I	☑
DTIC TAB	☐
Unannounced	☐
Justification	
By	
Distribution /	
Availability Codes	
Dist	Avail and / or Special
A-1	20

Published in *Microwave Journal*, Vol. 32, No. 9, Sep 1989.

14. SUBJECT TERMS

15. NUMBER OF PAGES

16. PRICE CODE

17. SECURITY CLASSIFICATION OF REPORT	18. SECURITY CLASSIFICATION OF THIS PAGE	19. SECURITY CLASSIFICATION OF ABSTRACT	20. LIMITATION OF ABSTRACT
UNCLASSIFIED	UNCLASSIFIED	UNCLASSIFIED	UNLIMITED

Detection of Covert Message Transmissions*

Robin A. Dillard and **George M. Dillard**
Naval Ocean Systems Center
San Diego, CA

Introduction

In this paper we describe and compare methods of detecting short, randomly occurring messages. The emphasis is on spread-spectrum transmissions, but the energy detection results also apply to simple burst communications, such as those used for interrogation or identification among network elements.[1]

A historical account of spread-spectrum systems is given in Scholz.[2] Some early papers concerning implementation have been reprinted[3]. Dixon's book[4] is a good introduction to spread-spectrum techniques. Pickholtz et al.[5] provide a tutorial treatment of the theory. A three-volume set by Simon et al.[6] includes a chapter on the detection of low probability of intercept (LPI) signals. Torrieri[1] covers secure communications and discusses the intercept problem. Schleher[7] includes a discussion of the detectability of LPI waveforms. Wiley[8] covers methods of intercepting radar LPI waveforms. Dillard and Dillard[9] address the detection of spread-spectrum signals. Several journal papers[10-14] outline techniques for detecting LPI signals.

Signal Structures

Figure 1 illustrates the use of notation and terminology. The duration and bandwidth of the transmission are denoted by T_1 and W_1. For hopped time or frequency transmissions, the duration and bandwidth of the frequency-hopped pulses, or data symbols, are T_2 and W_2. In a pure frequency-hopped (FH) transmission, the data symbol is a simple pulse ($T_2W_2 \approx 1$), and the pulses are contiguous in time. In a pure time-hopped (TH) transmission, the data symbol is a simple pulse and all occupy the same frequency band ($W_1 = W_2$). The duration of the TH-interval is denoted by T_p. Pseudonoise (PN) is a wideband, noise-like transmission. A pure PN transmission would fill the area $T_1 x W_1$. A hybrid signal is a combination of two or more spread-spectrum techniques. The most common are FH/PN, FH/TH, TH/PN, and FH/TH/PN.

The number of data symbols, or pulses, in a hopped transmission is denoted by b, with $b = T_1/T_2$ in an FH or an FH/PN transmission and $b = T_1/T_p$ in a TH, TH/PN, or FH/TH/PN transmission. The signal energy of the transmission is E_1 and the energy of each data symbol is $E_2 = E_1/b$.

The primary detection technique useful against weak PN and burst signals is energy detection. If the transmission involves hopped signals, then additional detection techniques should be considered. A wideband energy detector that integrates energy over the entire transmission is often the best choice.

Energy Detection

Ideal energy detection is described by the equation

$$V(t) = \int_{t-T}^{t} y^2(r)dr \qquad (1)$$

where y(t) is the input voltage, V(t) the output voltage, and T the integration time. When used in an integrate-and-dump (ID) mode, the output of the integrator is sampled every T seconds and then reset to zero. If two overlapping integrators are used with one filter, then a decision is made every T/2 seconds for that filter. In the case of continuous integration, the output from the integrator at any time t is the energy integrated over the time interval (t-T,t). Digital integration can provide a constant weighting with time when continuous integration is desired, but usually with a small degradation.[15]

Filter-Bank Energy-Detection Systems

A filter-bank energy-detection system is effective when the frequency band of each transmission, such as a burst, varies from transmission to transmission. It is also effective against hopped-frequency pulses. Against FH and FH hybrid transmissions where the possible frequencies are known, a bank of bandpass filters can be used to cover the frequency range, matching the filter bandwidth W to the bandwidth W_2 of the data symbols.

In the simplest filter-bank system, each filter is followed by an energy detector and a thresholder. While the system is modeled this way, the implementation may be more com-

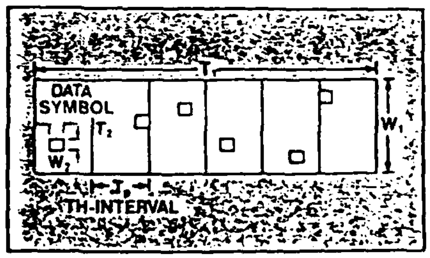

Fig. 1 An illustration of a signal-parameter notation.

*Invited paper.

plicated. For example, an RF spectrum analyzer implemented by using an acousto-optic Bragg cell with an exposed film strip as the output can function as a continuously integrating bank of energy detectors, one filter for each of a number of frequency bands.[16] An example of an I+D system is a Bragg cell spectrum analyzer that uses an array of photosensors containing photosites that are sampled (read out) and then cleared.[17] Schleher[7] describes a Bragg cell system that uses photodiode arrays coupled to charge-coupled devices for readouts. Performance standards for Bragg cell receivers are introduced in Tsui et al.[18]

Energy Detection Calculations

When an energy detector is used to integrate the energy of the entire transmission, the integration time should be $T = T_1$ and the passband of the filter should match the transmission band, with bandwidth $W = W_1$. Calculations for pulse-detection systems use the concept of dividing the time-frequency space under surveillance into cells of energy integration. This defines a grid of cells, each cell having area $TW = T_2W_2$. An ideal fit of the grid to the signal results in only two kinds of integration cells, cells containing signal energy and cells empty except for noise.

To analyze energy detection, we assume that the noise at the input to the energy detector is a zero-mean, stationary, Gaussian random process that has a flat, band-limited power spectral density. For large TW, we assume that an ideal rectangular-passband filter of bandwidth W precedes the energy detector. When TW is in the region of unity, the received signal energy depends on the pulse shape and filter shape. The normalized decision statistic V' is related to the integrated energy V by $V' = 2V/N_{01}$, where N_{01} denotes the one-sided noise power spectral density.

The thresholder compares the value of V' with a threshold K, and the decision is "signal present" if $V' \geq K$, and "noise only" if $V' < K$. For continuous integration, V' is the value of the normalized integrated energy

$$V'(t) = \frac{2}{N_{01}} \int_{t-T}^{t} y^2(r)dr \tag{2}$$

at any particular instant t. For I+D detection, the decision times are at instants T seconds apart. The false-alarm probability per decision is

$$Q_F = \text{Prob}[\, V' \geq K \text{ at time t}|\text{ no signal energy in } (t-T, t)] \tag{3}$$

and the detection probability per decision is

$$Q_D = \text{Prob}[\, V' \geq K \text{ at time t}|\text{ signal energy } E_S \text{ in } (t-T, t)]. \tag{4}$$

The vertical bar | indicates that the probability is conditional on the

(Continued on page 140)

event following the bar.

The distribution function of the test statistic V' is closely approximated by the chi-square distribution with 2TW degrees of freedom in the noise case and by the noncentral chi-square distribution with 2TW degrees of freedom and noncentrality parameter $\lambda = 2E_S/N_{01}$ in the signal case.[1,10] For TW = 1, the distribution is equivalent to the square-law form of the Rice distribution, which describes envelope detection of a single pulse. When TW is any integer, the equation for Q_D is the generalized Q-function, $Q_D = Q_{TW}(\sqrt{2S}, \sqrt{K})$, where $S = E_S/N_{01}$ is the signal-to-noise ratio (SNR).[10]

The value of the bias level, the normalized threshold $K_0 = K/2$, that provides the desired Q_F is found in Pachares' table[19] for TW = 1,2,. . .,150, and for $Q_F = 10^{-P}$, P = 1,2,. . .,12. A technique outlined by Helstrom[20] can be used to approximate K_0 for moderately large values of TW, such as, for TW > 20.

Robertson[21], Dillard[22], and Parl[23] give recursive formulas for computing Q_D. Helstrom[20] gives techniques for an approximate evaluation. This approximation and others are discussed below.

Energy Detection Approximations

For large values of TW, the central limit theorem can be used to obtain normal approximations to Q_F and Q_D.[10] In terms of the normal cumulative distribution function

$$F(y) = \frac{1}{\sqrt{2\pi}} \int_{-\infty}^{y} e^{-z^2/2} dz \qquad (5)$$

the approximations are

$$Q_F \approx 1 - F[(K_0 - TW)/\sqrt{TW}] \qquad (6)$$

and

$$Q_D \approx 1 - F[(K_0 - TW - S)/\sqrt{TW + 2S}]. \qquad (7)$$

By solving Equation 6 for the normalized threshold K_0 we obtain

$$K_0 \approx F^{-1}(1 - Q_F)\sqrt{TW} + TW, \qquad (8)$$

where $F^{-1}(x)$ is equal to the variate y such that F(y) = x. Substitution of Equation 8 into Equation 7 yields

$$Q_D \approx 1 - F\{[F^{-1}(1 - Q_F) - S/\sqrt{TW}]/\sqrt{1 + 2S/TW}\}. \qquad (9)$$

The approximation in Equation 9 is called the "full normal approximation". A further approximation valid for S<< 2TW is

$$Q_D \approx 1 - F[F^{-1}(1 - Q_F) - S/\sqrt{TW}]. \qquad (10)$$

The approximations given by Equation 9 and Equation 10 for energy detection require the product TW to be large, but their accuracy also depends on the values of

[Continued on page 144]

Q_F and Q_D. Equation 7 provides a good approximation to Q_D when the value used for K_0 is accurate, even for relatively small values of TW, such as, TW=20 or larger. Equations 9 and 10 are in error primarily because the approximation to K_0 in Equation 8 is in error.

If K_0 is known, we can use Equation 7 to estimate the SNR required to achieve a given value of Q_D. The estimate is

$$\hat{S} = K_0 - TW + \gamma^2 - \gamma\sqrt{2K_0 - TW + \gamma^2} \quad (11)$$

where $\gamma = F^{-1}(1-Q_D)$.[9] When $Q_D = 0.5$, then $\gamma = 0$, and the estimate is

$$\hat{S}(0.5) = K_0 - TW. \quad (12)$$

Equation 11 is obtained by solving the quadratic equation $K_0 - TW - S = \gamma\sqrt{TW + 2S}$ for S. Note from Equation 12 that the difference $K_0 - TW$ is an estimate of the required SNR for Q_D=0.5.

The two normal approximation Equations 9 and 10 and the "hybrid" approximation using Equation 7 and the true K_0 are compared with the "exact" results (using the noncentral chi-square distribution) in Figure 2 for $Q_F = 10^{-12}$. The hybrid approximation gives results equal to the exact results except for small TW, where none of the approximations are reasonable. Therefore, if the true values of K_0 are available, there is no need to use Equation 9 or 10. Evaluation of Equation 7 using Hasting's approximations[24] is much simpler than evaluation of the noncentral chi-square distribution using,[21-23] rather than the approximation using Helstrom's technique.[20]

False-Alarm Rate

The false-alarm rate (FAR) for a single-filter energy-detection system with simple thresholding is the product of the decision rate and the false-alarm probability Q_F. For I+D detection, the decision rate is 1/T; for overlapping I+D detection, it is 2/T. The FAR for the filter-bank system with simple thresholding is

FAR = (number of filters) x (decision rate per filter) x Q_F.

For I+D detection, we then have $FAR = NQ_F/T$, where N is the number of filters. In Figure 3, the FAR is held constant with changing TW by fixing the value of Q_F/TW. Note the misleading fact that Q_D improves as TW increases when computations stray into the area where Q_D is less than 10 Q_F. When integration is over the entire transmission, the message detection probability is $P_d = Q_D$. When integration is over individual data symbols, the message detection probability is a function of Q_d and b. Figure 3 applies to both cases. Curves for other false-alarm rates are given in Reference 9.

Splitting Loss

For I+D detection, matching the integration time to the signal duration is optimum only if the integration interval coincides with the signal. In practice, the signal is likely to be split into two intervals of integration. Figure 4 gives an example of the effect on detection probability, for TW ≈ 1. The average detection probability is $1 - [1 - Q_D(xE)][1 - Q_D(E - xE)]$ averaged over x, where x is uniformly distributed between 0 and 0.5. Figure 5 gives the loss L_t corresponding to the average detection probability for several combinations of TW and Q_F.

Mismatched Integration Time

If the integration interval significantly exceeds the duration of the signal, a loss results from the unnecessary integration of additional noise power. A small offset to this loss is the decreased splitting loss. If the integration time is significantly less than the signal duration, then detection involves "repeated observations". For message duration T_1, one computes Q_D for $E_S = E_1T/T_1$ and lets the message detection probability equal

$$P_d \approx 1 - (1 - Q_D)^{T_1/T} \quad (13)$$

[Continued on page 146]

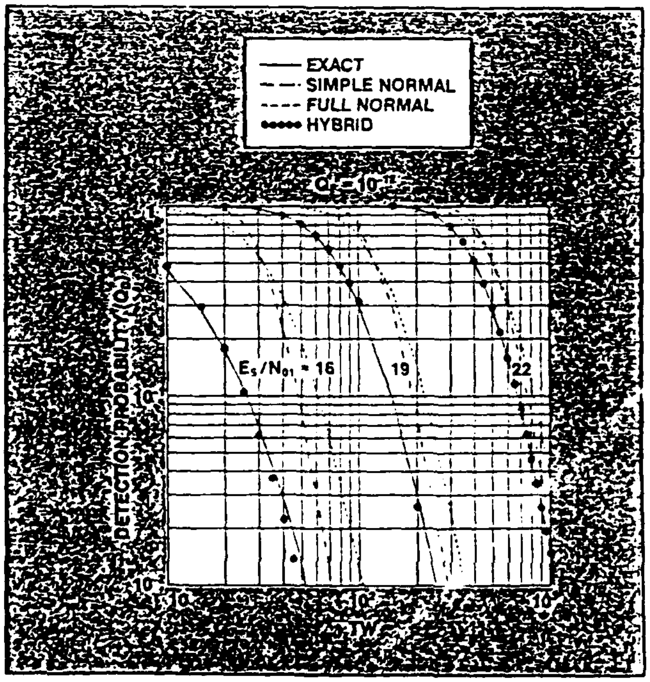

Fig. 2 Comparison of approximations with exact distribution.

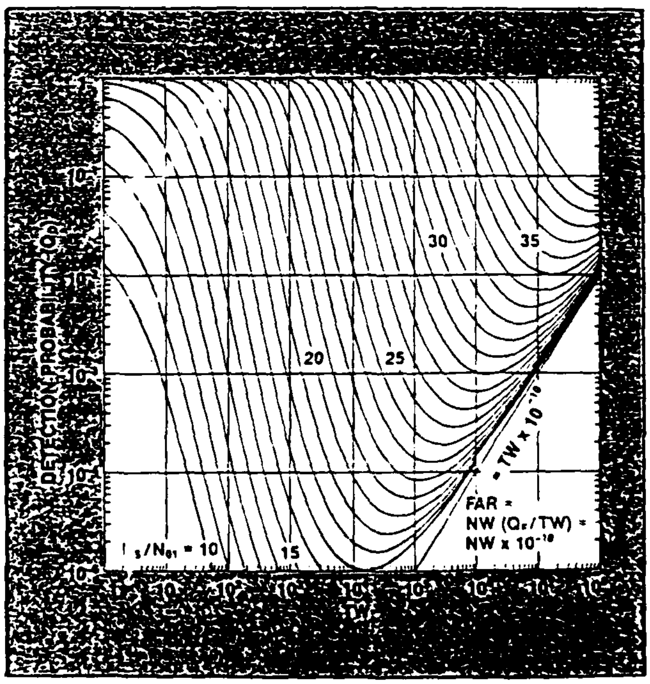

Fig. 3 Detection probability per integration for a fixed FAR.

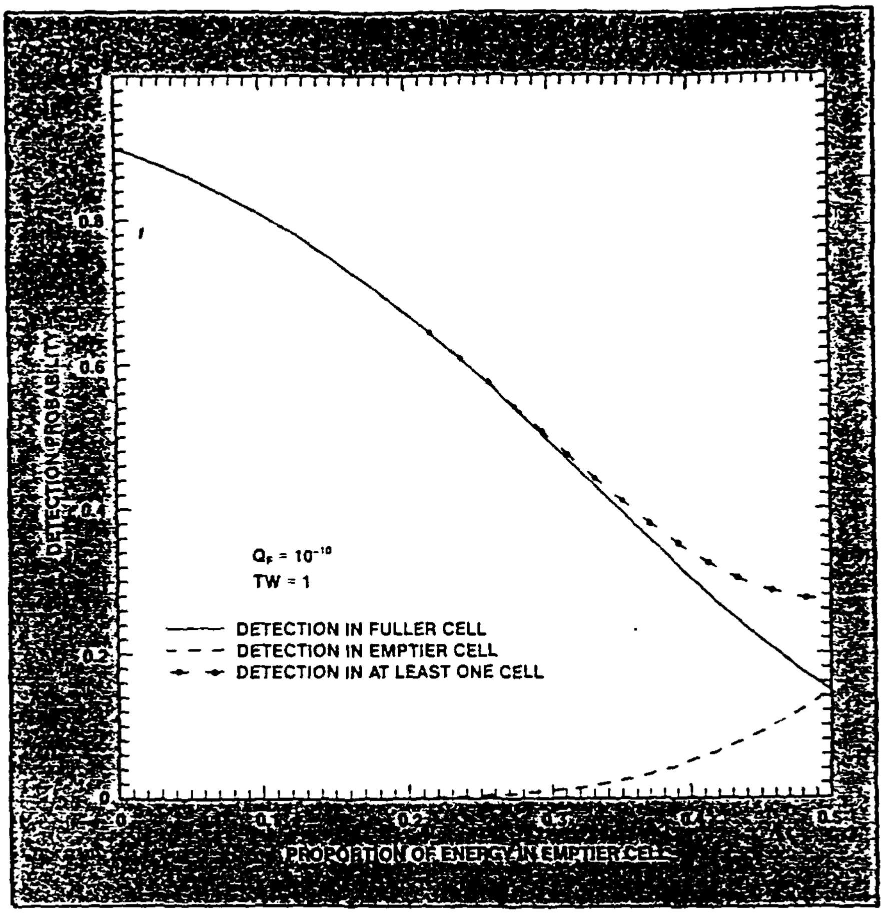

Fig. 4 Example of splitting signal energy into two time intervals of energy integration.

Splitting loss applies only to the first and last integration of signal energy.

Figure 6 gives an example of the loss for both kinds of mismatching, for a fixed message size ($T_1W_1 = 10^4$) and for varying T, with $W = W_1$. Recall that Q_F varies with T for a fixed FAR. *Figure 7* shows the average loss, which varies only slightly with TW, Q_F, and Q_D.

Energy Integration over Each Data Symbol

Consider a hopped transmission consisting of b data symbols. The data symbols can be simple pulses ($T_2W_2 \approx 1$; as in FH, TH, or FH/TH), or can have a PN microstructure ($T_2W_2 >> 1$; as in FH/PN, TH/PN, or FH/TH/PN). The detection system is modeled by a bank of N filter-detector-thresholder units, where N = 1 for TH or TH/PN. By using the grid concept, there are b cells containing signal energy and m noise-only cells in the period of length T_1, where

$$m = N \frac{T_1}{T_2} - b \tag{14}$$

If a signal decision in one of the m empty cells leads to an examination of the message in a recognition stage, then P_d is the probability that a threshold-crossing occurs during the message arrival time. For an ideal grid fit, we have

$$P_d = 1 - (1 - Q_D)^b \ (1 - Q_F)^m \tag{15}$$

where Q_D is the probability of detecting a data symbol. The approximation

$$P_d \approx 1 - (1 - Q_D)^b \tag{16}$$

[Continued on page 148]

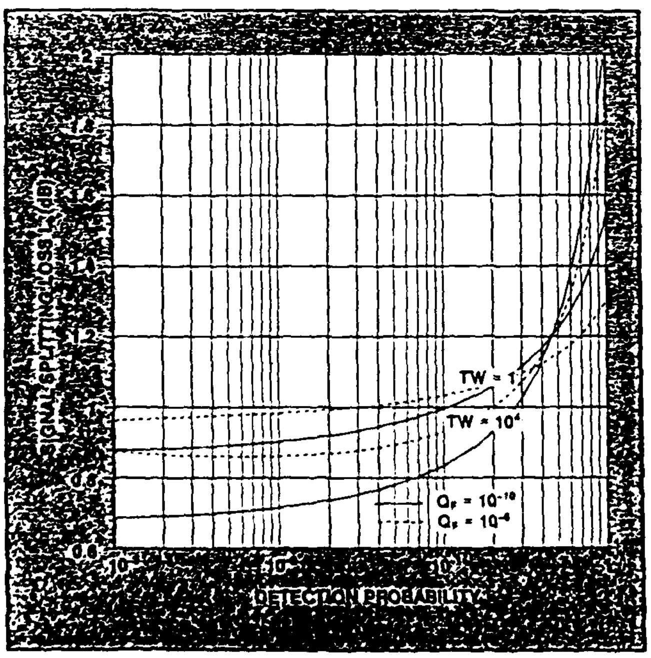

Fig. 5 Loss as a function of the probability that the signal is detected in at least one cell averaged over all splitting proportions.

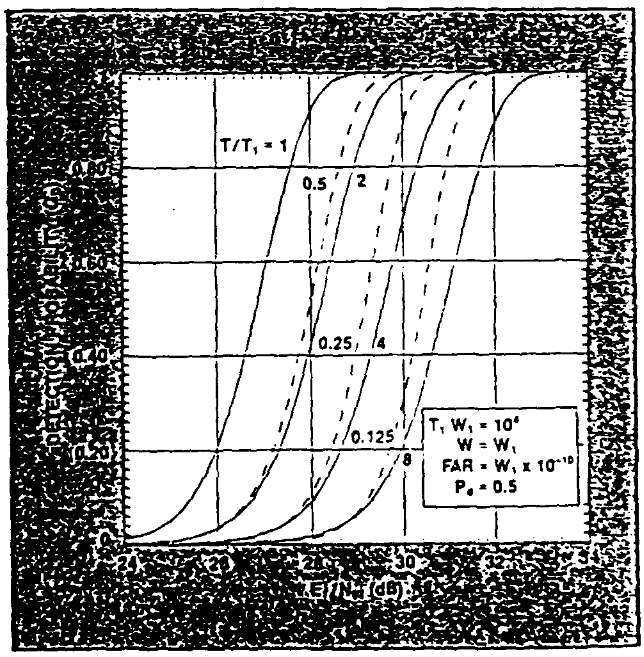

Fig. 6 Illustration of result of mismatching the integration interval T with the signal duration T_1.

is usually valid. Note, however, that if Q_D is close to Q_F, (15) gives $P_d \approx bmQ_F$ while Equation 16 gives $P_d \approx bQ_F$, and these can differ by orders of magnitude.

The results above assume that each data symbol is contained entirely in some time bandwidth cell of integration. The loss L_f resulting from a random splitting of the signal into two adjacent passbands can be taken into account when estimating the received energy E_2. A loss L_t occurs for I+D detection when the signal is split randomly into two integration intervals. For PN data symbols, losses L_f and L_t are approximately equal to each other and are additive.[9]

Binary Moving-Window Detection

A binary moving-window detector (BMWD)[25] implements the requirement that at least k out of b pulses be detected for a "signal present" decision to be made. In the applications here, some of the detections result from noise in otherwise empty time-bandwidth cells.

First, consider the use of a BMWD system against TH or TH/PN signals. An energy detector (with integration time $T = T_2$) followed by a thresholder provides the input to the BMWD. Every T_2 seconds the input is a 0 or a 1. (A run-suppressor unit is also needed, because the integration interval is not synchronized with pulse times.) The binary integration time is T_M, usually the message duration, T_1. At each time jT_2, the BMWD computes the test statistic

$$S_j = \sum_{k=j-M+1}^{j} y_k \qquad (17)$$

and compares it with a threshold K_M. The window length is M, where $M = T_M/T_2$. An alarm occurs when the test statistic S_j reaches the threshold K_M in an upward direction.

If synchronization with the hopping intervals of a TH or TH/PN transmission were possible, the knowledge that one and only one data symbol occurs in each TH interval could be used by employing a binary-tapped delay-line and an OR-gate. The output of the OR-gate every T_p seconds would then be $y_k = 0$ if every slot in the TH-interval yields 0, and would be 1 otherwise. Computations for this synchronized case give a close upper boundary to the detection capability of pulse-detection systems against a TH or TH/PN transmission, and are much simpler than for the unsynchronized case.

Against FH, FH/PN, FH/TH, and FH/TH/PN transmissions, a filter-bank BMWD system can use the knowledge that only one frequency slot is occupied at any instant by employing an OR-gate to allow, at most, a single "1" to enter the window every T seconds. The synchronization assumption also can be applied to filter-bank BMWD systems for detecting FH/TH and FH/TH/PN transmissions. In the latter case, the BMWD accepts a single 1 or 0 from each block of NT_p/T_2 cells.

The probability, at any time jT_2 that the binary number 1 enters the BMWD is denoted by p_0 when only noise is present during the previous T_2 seconds, and is denoted by p_1 when a signal is present (in one of the N passbands). For the single-filter system (unsynchronized with the TH-interval), the formulas for p_0 and p_1 are simply $p_0 = Q_F$ and $p_1 = Q_D$. For the filter-bank system with an OR-gate applied to the N filter-detector-thresholder inputs, the formulas are

[Continued on page 150]

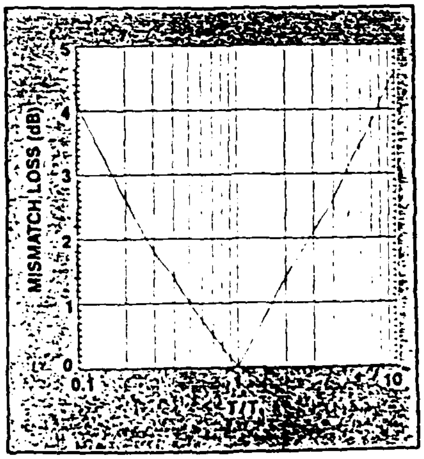

Fig. 7 Loss resulting from mismatching the integration interval with the signal duration averaged over a range of parameter combinations.

[From page 148] DILLARD

$$p_0 = 1 - (1-Q_F)^N \qquad (18)$$

and

$$p_1 = 1 - (1-Q_F)^{N-1}(1-Q_D) \qquad (19)$$

At each time jT_2, the BMWD computes S_j, given by Equation 17, and compares it with the threshold K_M, where $M = T_1/T_2$ is the window length. The system alarms when the sum S_j reaches the threshold K_M in an upward direction, such as, when $S_{j-1} = K_M-1$ and $S_j = K_M$. The probability of this joint event when no signal is present is

$$P_T = \binom{M-1}{K_M - 1} p_0^{K_M}(1 - p_0)^{M-K_M+1} \qquad (20)$$

The FAR, in alarms per second, is $FAR = P_T/T_2$.

The probability of a detection by the BMWD is approximately equal to (and bounded below by) the probability that there are at least K_M 1s in the window when the window is aligned in time with the transmission. This probability is[11]

$$P_d = \sum_{i=K_M}^{M} \sum_{j=\max(0,i-M+b)}^{\min(i,b)} \binom{b}{j}\binom{M-b}{i-j} p_1^j p_0^{i-j} \cdot (1-p_1)^{b-j}(1-p_0)^{M-i+j-b}. \qquad (21)$$

For FH or FH/PN, with M = b, Equation 21 becomes

$$P_d = \sum_{i=K_M}^{b} \binom{b}{i} p_1^i(1-p_1)^{b-i} \qquad (22)$$

Equation 22 also applies to systems assumed to have an OR function synchronized with the TH-interval, if we use

$$p_1 = 1 - (1-Q_F)^{NT_p/T_2-1}(1-Q_D). \qquad (23)$$

The window length is M=b, and the FAR becomes $FAR=P_T/T_p$, where the computation of P_T uses

[Continued on page 152]

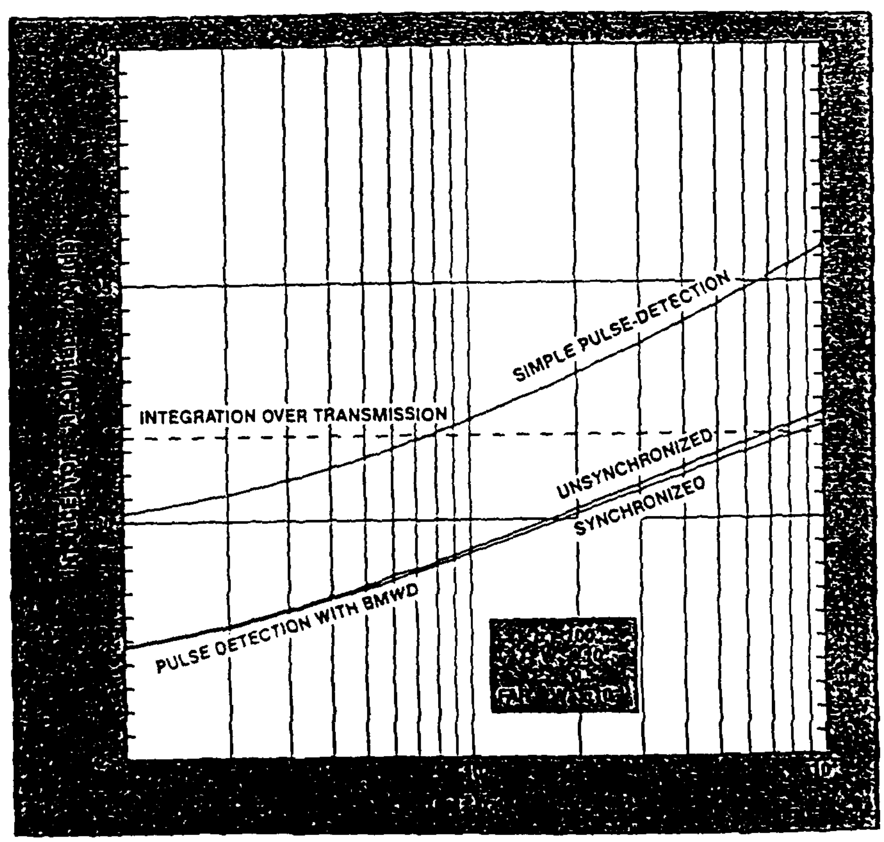

Fig. 8 A comparison of pulse detection systems for TH/PN transmissions.

[From page 150] DILLARD

$$p_o = 1 - (1 - Q_F)^{NT_p/T_2}. \quad (24)$$

For the unsynchronized systems used against signals involving TH, the use of Equation 22 with Equation 23 serves as a good approximation to Equation 21. For fixed FAR and E_2, it provides an upper boundary to Equation 21 when Equation 24 is used with M = b and FAR = P_T/T_p, and a lower boundary to Equation 21 when Equation 18 is used with M = bT_p/T_2 and FAR = P_T/T_2. The value of Q_F, and therefore of p_1, is different for the two calculation methods.

Comparisons of Detection Methods

Against hopped transmissions, the dedicated interceptor must determine whether integration over the transmission (IOT) or integration over individual data symbols (pulse detection) is better. If the pulse-detection approach is competitive, then additional signal-processing techniques, such as BMWD should be considered. Generally, IOT is better when signal energy densely occupies the transmission's time-bandwidth area and pulse-detection is better when pulses are sparsely distributed.

Against TH/PN signals, the size T_2W_2 of the data symbols strongly affects pulse-detection performance, as illustrated in Figure 8. Note that IOT becomes better than pulse detection as T_2W_2 increases.

Figure 9 compares systems for two FH cases, one where only ten frequencies are used and one where 10^4 are used. Note that, for 10^4 frequencies, IOT becomes better than simple pulse detection when b exceeds 3000, and better than BMWD with OR-gating when b exceeds 10^4.

The results shown in Figure 8 for TH/PN and in Figure 10 for FH are reflected in Figure 10, which considers IOT detection vs. pulse detection with BMWD. The upper left area corresponds to sparse signal occupancy, and the area under the curves corresponds to dense occu-

[Continued on page 154]

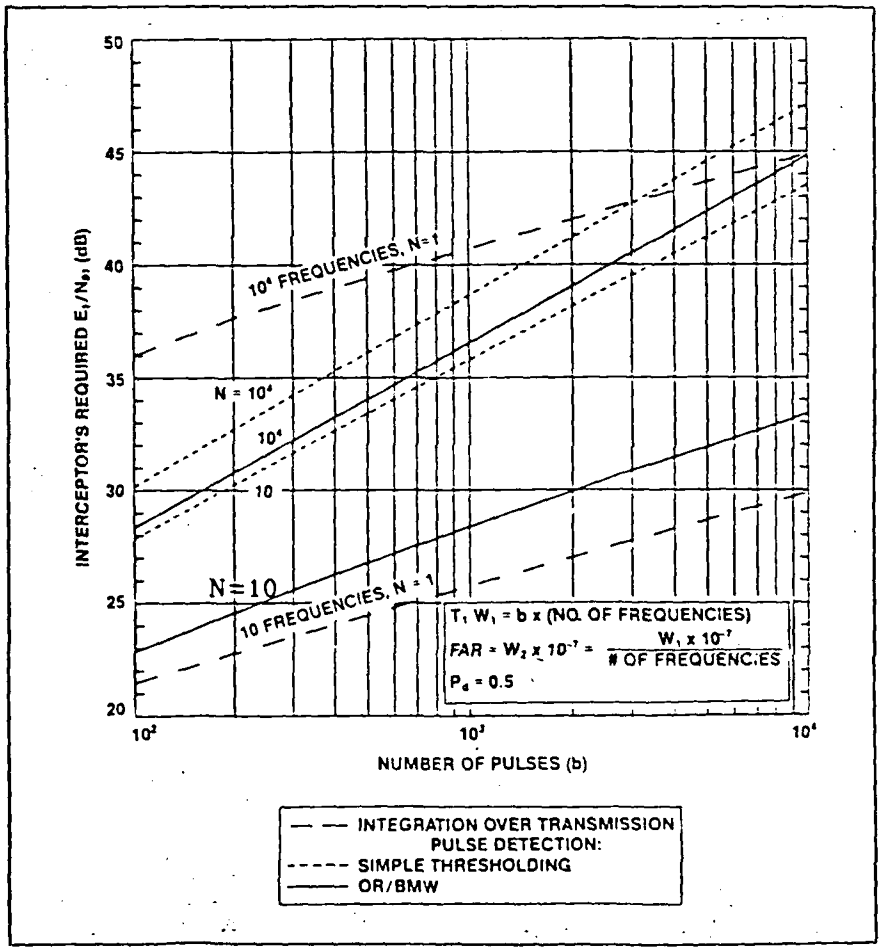

Fig. 9 A comparison of detection methods for pure FH, N filters.

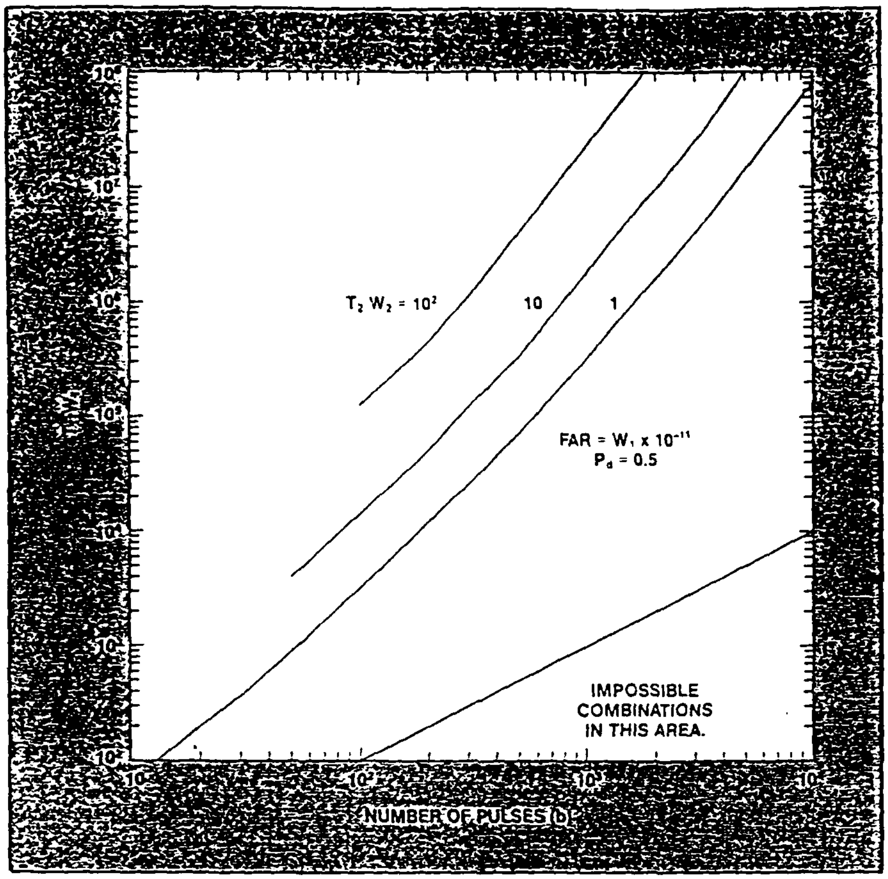

Fig. 10 For combinations of T_1 W_1 and b that fall above the curve corresponding to the selected pulse size, pulse detection using a BMWD is the better detection method. Below the curve, integration over the transmission is better.

pancy. For intermediate values of signal density, the designer of the detection system should use the formulas given here or use graphs[9] to determine whether to integrate the signal energy over the entire message or to use a pulse-detection system. ■

References

1. D.J. Torrieri, *Principles of Secure Communications Systems*, Norwood, MA, Artech House, 1985.
2. R.A. Scholz, "The Origins of Spread-Spectrum Communications," IEEE Trans. on Comm., Vol. COM-30, May 1982, pp. 822-854.
3. R.C. Dixon, ed., *Spread Spectrum Techniques*, New York, IEEE Press, 1976.
4. R.C. Dixon, *Spread Spectrum Systems*, Second Edition, New York, John Wiley & Sons, 1984.
5. R.L. Pickholtz, et al., "Theory of Spread-Spectrum Communications," IEEE Trans. on Comm., Vol. COM-30, May 1982, pp. 855-884.
6. M.K. Simon, et al., *Spread Spectrum Communications*, Vol. I-III, Rockville, MD, Computer Science Press, 1985.
7. D.C. Schleher, *Introduction to Electronic Warfare*, Norwood, MA, Artech House, 1986.
8. R.G. Wiley, *Electronic Intelligence: The Interception of Radar Signals*, Norwood, MA, Artech House, 1985.
9. R.A. Dillard and G.M. Dillard, *Detectability of Spread-Spectrum Signals*, Norwood, MA, Artech House, 1989.
10. H. Urkowitz, "Energy Detection of Unknown Deterministic Signals," Proc. IEEE, Vol. 55, April 1967, pp. 523-531.
11. R.A. Dillard, "Detectability of Spread-Spectrum Signals," IEEE Trans. on AES, Vol. AES-5, July 1979, pp. 526-537.
12. N.F. Krasner, "Optimal Detection of Digitally Modulated Signals," IEEE Trans. on Comm., Vol. COM-30, May 1982, pp. 885-895.
13. A. Polydoros and C.L. Weber, "Optimal Detection Considerations for Low Probability of Intercept," MILCON '82 Conference Record, Vol. 1, 1982, pp. 2.1-1 to 2.1-5.
14. A. Polydoros and C.L. Weber, "Detection Performance Considerations for Direct-Sequence and Time-Hopping LPI Waveforms," IEEE Trans. on Selected Areas in Comm., Vol. SAC-3, September 1985, pp. 727-744.
15. J.E. Ohlson, "Efficiency of Radiometers Using Digital Integration," *Radio Science*, Vol. 6, No. 3, May 1970, pp. 341-345.
16. N.J. Berg and J.N. Lee, eds., *Acousto-Optic Signal Processing*, New York, Marcel Dekker, Inc., 1983.
17. T.M. Turpin, "Spectrum Analysis Using Optical Processing," Proc. IEEE, Vol. 69, No. 1, Jan. 1981, pp. 79-92.
18. James B. Tsui, et al., "Performance Standards for Wideband EW Receivers," *Microwave Journal*, Feb. 1989, pp. 46-54.
19. J. Pachares, "A Table of Bias Levels Useful in Radar Detection Problems," IRE Trans. on Inf. Theory, Vol. IT-4, March 1958, pp. 38-45.
20. C.W. Helstrom, "Approximate Evaluation of Detection Probabilities in Radar and Optical Communications," IEEE Trans. on AES, Vol. AES-14, No. 4, July 1978, pp. 630-640.
21. G.H. Robertson, "Computation of the Noncentral Chi-Square Distribution," Bell System Tech. Journal, Vol. 48, Jan. 1969, pp. 201-207.
22. G.M. Dillard, "Recursive Computation of the Generalized Q Function," IEEE Trans. on AES, Vol. AES-9, No. 4, July 1973, pp. 614-615.
23. S. Parl, "A New Method of Calculating the Generalized Q Function," IEEE Trans. on Inf. Theory, Vol. IT-26, No. 1, Jan. 1980, pp. 121-124.
24. M. Abramowitz and I.A. Stegun, Eds., *Handbook of Mathematical Functions*, National Bureau of Standards, AMS-55, Seventh Printing, p. 932, May 1968.
25. G.M. Dillard, "A Moving-Window Detector for Binary Integration," IEEE Trans. on Inf. Theory, Vol. IT-13, No. 1, Jan. 1967, pp. 2-6.

George M. Dillard *received his AB and BS degrees in mathematics form San Diego State College in 1959 and 1962, respectively, and his PhD degree in information and computer science from the University of California at San Diego in 1971. He has been employed at the Naval Ocean Systems Center since 1959 when it was known as the Navy Electronics Laboratory. His work has mainly involved signal detection analysis for radar, communications and electronic warfare systems. He is currently a staff scientist involved in the selection of projects for the NOSC Independent Research Program.*

Robin A. Dillard *received her AB degree in mathematics from San Diego State College in 1958. She has been employed at the Naval Ocean Systems Center since 1958 when it was known as the Navy Electronics Laboratory. Her work has mainly involved signal detection analyses for radar, communications and electronic warfare systems. During the last eleven years, much of her effort has been in the application of artificial intelligence (AI) techniques to decision problems in command, control and communications. Her current research and development activities include AI applications to RF network selection and to electronic warfare planning.*